Pergamon

Bioorganic & Medicinal Chemistry, Vol. 3, No. 3, pp. 321–335, 1995

0968-0896/95 $9.50 + .00

0968-0896(95)00029-1

Molecular Mechanics and Dynamics Studies on Two Structurally Related Amide-Modified DNA Backbones for Antisense Technology

Valérie Fritsch, Alain De Mesmaeker, Adrian Waldner, Jacques Lebreton, Marcel J. J. Blommers and Romain M. Wolf*

Central Research Laboratories, Ciba-Geigy Ltd, CH-4002 Basel, Switzerland

Abstract—The effect of the replacement of the natural phosphodiester linkage -C3'-O-PO_2^--O-CH_2-C4'- in the DNA strand of RNA·DNA hybrid duplexes by either of the two amide linkages -C3'-CH_2-CO-NH-CH_2-C4'- or -C3'-CH_2-NH-CO-CH_2-C4' has been investigated by molecular mechanics (MM) and molecular dynamics (MD) simulations. Conformational analysis has been used to assess various low-energy conformers of the amide-modified backbones. MD simulations have been carried out to study the dynamic behavior of the modified duplexes. The modified RNA·DNA hybrid double helices kept a conservative base pairing scheme during the MD simulations. Although the general behavior has been found to be similar to that of the corresponding wild-type hybrid duplexes, some notable differences, especially regarding the sugar puckering in the amide-modified DNA strands, have been observed. The behavior of the RNA strands in the hybrid duplexes has not been affected by the modified DNA strands and is similar to that in wild-type RNA·DNA duplexes.

Introduction

Antisense oligo(deoxy)nucleotides constitute a new class of antiviral drugs promising a selective chemotherapeutic strategy to treat human diseases.[1–3] Synthetic modifications of oligo(deoxy)nucleotides are required in order to use them in antisense technology.[4–7] The binding affinity and specificity for the RNA target should be maintained compared to the natural phosphodiester backbone. Simultaneously however, the stability of the antisense oligonucleotides toward nucleases and their cellular uptake should be increased.

Among the various possibilities for chemically modifying the structure of oligonucleotides, modifications to the nucleic acid backbones, in particular substituting the phosphodiester, have turned out to be especially promising.[6,7] The phosphodiester linkage is the point of attack of nucleases and its charge is mainly responsible for the low cell penetration of natural oligonucleotides.

Recent studies in our laboratories have focused on the design and preparation/synthesis of dimers with neutral amide linkages connecting two deoxyribonucleosides.[8–13] All five chemically stable structural isomers of amide-linked deoxyribonucleosides shown in Figure 1 were synthesized and incorporated into various DNA sequences. Modified oligonucleotides with one or several amide linkages were found to form stable and specific duplexes with complementary wild-type RNA strands. The melting points of these duplexes for amides **1**, **2** and **5** were slightly lower than those of the corresponding wild-type hybrid duplexes.[8,9,12] However, modifications giving amide **3** and amide **4** had a stabilizing effect in several sequences (up to 0.9 °C per modification).[10,11] We have used computer simulations to elucidate the possible changes in the supramolecular structures of RNA·DNA duplexes induced by the replacement of some phosphodiester linkages by amide moieties. The theoretical studies should serve as a basis for understanding the structural features and for the possible design of further modifications. This publication

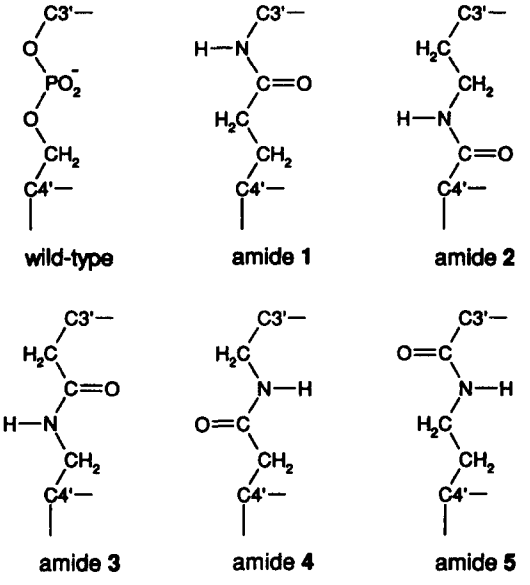

Figure 1. Wild-type phosphodiester linkage and the five chemically stable structural isomers of amide linkages proposed as a substitute for the phosphodiester in antisense oligodeoxynucleotides.

reports on molecular modeling results obtained for the amide **3** and amide **4** modifications which can be regarded as structural isomers of the same hypothetical double bond. The investigations include conformational analysis to find low-energy conformers of the amide-modified backbone segments and molecular dynamics studies to investigate possible fluctuations and transitions. Computer simulation results concerning the three other modifications will be published elsewhere.

Computational Methods

General settings

All calculations were carried out with the AMBER[14] all-atom force field as incorporated in the software package Insight 2.2.0/Discover 2.9 from BIOSYM Technologies, San Diego, U.S.A. The computations were run on a Silicon Graphics Crimson workstation. The potential energy function includes harmonic terms for covalent structure deformation (bond and bond angle deformations), an intrinsic torsional potential term, and pairwise interaction terms for the nonbonded interactions, i.e. van der Waals, electrostatic and hydrogen bonding terms:

$$E_{total} = \sum_{bonds} \frac{k_l}{2}[l - l_0]^2 + \sum_{angles} \frac{k_\theta}{2}[\theta - \theta_0]^2 + \sum_{torsions} \frac{V_n}{2}[1 + \cos(n\phi - \phi_0)] + \sum_{i=1}^{N}\sum_{j>i}^{N} 4\varepsilon_{ij}\left[\left(\frac{\sigma_{ij}}{r_{ij}}\right)^{12} - \left(\frac{\sigma_{ij}}{r_{ij}}\right)^{6}\right] + \sum_{i=1}^{N}\sum_{j>i}^{N}\left[\frac{332\,\delta_i\delta_j}{\varepsilon r_{ij}}\right] + \sum_{H\text{-}bonds}\left[\frac{C_{ij}}{r_{ij}^{12}} - \frac{D_{ij}}{r_{ij}^{10}}\right] \quad (1)$$

As suggested by Weiner *et al.*,[15] the 1–4 nonbonded interactions (i.e. interactions between atoms separated by 3 consecutive bonds) were scaled down by a factor of 2. To allow for the solvent and counterion screening effect, a distance-dependent dielectric function $\varepsilon = 4 \cdot r_{ij}$ was used for the electrostatic-energy calculation. This approach has been shown to lead to reasonable results in various systems despite the obvious lack of detailed interatomic interactions with water.[16–18] Some simulations including explicit water molecules and counterions are currently being carried out. They have been limited to octamer duplexes (with one amide modification in the middle) so far. The preliminary results from these extended simulations do not indicate major divergences from the conformational behavior reported here for the larger duplex structures. A full account on these investigations will be reported elsewhere.

Partial charges, atom types and starting geometries

Partial charges were assigned by a "donor–acceptor" scheme (T. Thacher, BIOSYM Technologies, unpublished work) fitting as closely as possible original AMBER charges where applicable. It was verified that the use of these partial charges in simulations on unmodified duplexes (used as reference structures for this work) produced results identical to those obtained with the original AMBER partial charges.[19] Figure 2 depicts the partial charges used for the unmodified backbone, sugars and bases. Partial charges specific to the amide-modified backbone portions are given in Figure 3.

All atom types required for the amide-modified sequences are defined in the original AMBER force field. Also, no additional force field parameters are needed. It is important to note that the potential energies will not be comparable between amide **3** and amide **4** modifications because not all torsional angles are defined by the same atoms. Therefore, only energies between different conformations of the same modification can be compared directly.

Starting structures for modified and unmodified RNA·DNA duplexes were built using the default settings in the Biopolymer module of Insight 2.2.0. Both strands were in a standard A-form with RNA and DNA sugars in an initial C3'-*endo* puckering state. To describe the sugar puckering behavior, we shall hereafter use the phase angle of pseudorotation P and the maximum degree of puckering τ_m calculated from the five endocyclic torsional angles as defined by Rao *et al.*[20] With this nomenclature, the C3'-*endo* puckering state corresponds to $P = 18°$, O4'-endo to $P = 90°$, and C2'-*endo* to $P = 162°$. In the case of nucleic acid furanoses, τ_m is usually close to 40°. Torsional angles, as shown in Figure 4, are defined according to IUPAC standards (see also Table 1).[21]

Conformational analysis

A detailed conformational analysis was carried out in order to assess possible conformations of the amide modified backbones and to generate adequate starting geometries for MD simulations. In a first step, an octamer hybrid duplex r(GA_6G)·d(CT_6C) was built in which the DNA–standard phosphodiester linkage between the central residues T4 and T5 was replaced by an amide-modified backbone (see Figure 4). Different conformers were then obtained by enforcing incrementally selected backbone torsional angles (see below). The enforcement was achieved by adding an additional harmonic term E_{enf} to the potential energy function to penalize any deviation from the required value:

$$E_{enf} = k_{enf}(\phi_{enf} - \phi)^2 \quad (2)$$

where k_{enf} is a force constant (chosen as 1000 kcal mol^{-1} rad^{-2}), ϕ_{enf} is the desired value of the torsional angle, and ϕ its actual value. In this way, various backbone conformations could be generated without disruption of the double-helix structure.

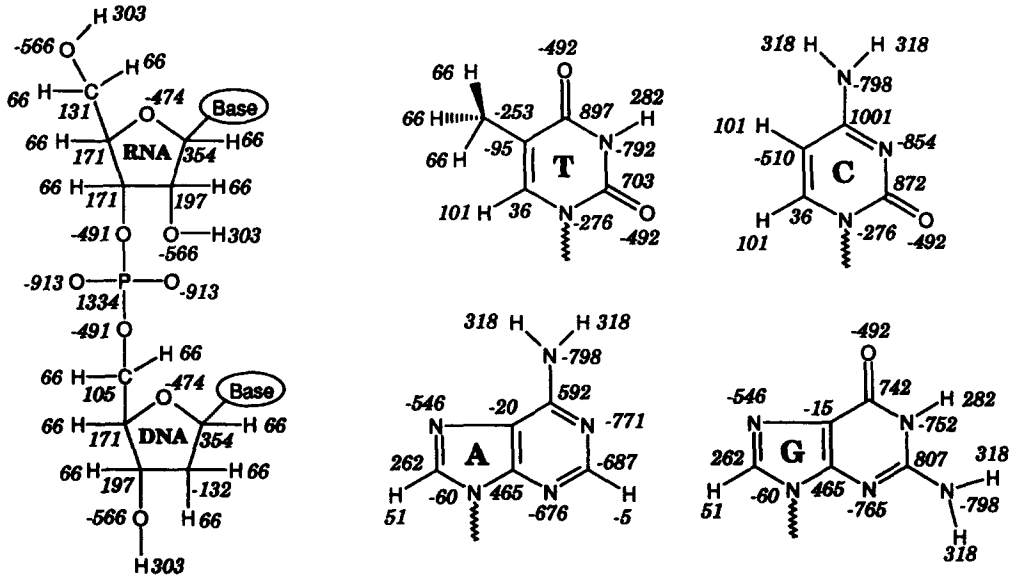

Figure 2. Atomic partial charges used for the unmodified DNA and RNA backbone, sugars and bases (elementary charges units $\times 10^3$). The charges are generated by donor–acceptor scheme (T. Thacher, BIOSYM Technologies, San Diego, U.S.A., unpublished work) and reproduce closely the original AMBER charges.[14]

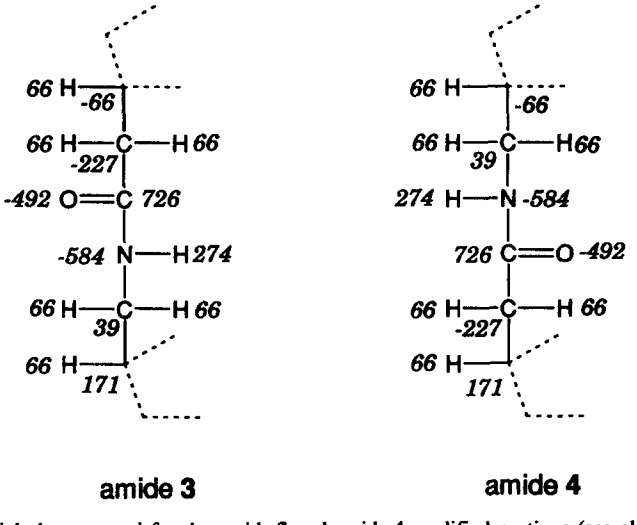

Figure 3. Atomic partial charges used for the amide 3 and amide 4 modified portions (see also legend of Figure 2).

Table 1. Backbone conformations[a] of local energy minima found for the amide 3 modified octamer r(GA$_6$G)·d(CTTT*TTTC)

Domain	Energy[b]	Residue	α	β	γ	δ	ε	ζ	χ	amide
3a	–139.2	i [c]	–75	177	60	77	**178**	**–79**	–157	*trans*
	(0.0)	i+1	**170**	**–157**	**166**	85	–155	–62	–169	
3b	–138.7	i	–74	178	59	75	**171**	**55**	-159	*trans*
	(+0.5)	i+1	**–172**	**73**	**170**	77	–158	–65	–171	
3c	–136.3	i	–75	176	58	71	**92**	**81**	–159	*trans*
	(+2.9)	i+1	**–171**	**157**	**71**	77	–173	–67	–148	
3d	–135.6	i	–76	177	58	75	**–172**	**–99**	–160	*cis*
	(+3.6)	i+1	**-3**	**134**	**49**	76	–163	–64	–160	

[a]Torsion angles are defined according to the IUPAC nomenclature:[21]
backbone: O3'-P-$^{\alpha}$-O5'-$^{\beta}$-C5'-$^{\gamma}$-C4'-$^{\delta}$-C3'-$^{\varepsilon}$-O3'-$^{\zeta}$-P-O5';
glycosidic angle χ: O4'-C1'-N9-C4 for purines, O4'-C1'-N1-C2 for pyrimidines.
For the modified residues, the same nomenclature is used with atoms O3'-P-O5' replaced by C-X-Y (see Figure 4). Torsion angles in bold refer to the modified portion C3'-CH$_2$-X-Y-CH$_2$-C4'.
[b]AMBER potential energy (in kcal mol^{-1}) of the modified octamer r(GA$_6$G)·d(CTTT*TTTC). Energy difference relative to the lowest-energy minimum is given in parentheses. Note that all energy values refer to the entire octamer duplex.
[c]The first line for each domain refers to the residue with the amide backbone portion attached at C3', the second line to the following residue with the modification attached to C4' (see Figure 4). In this case, residue i refers to T4 and residue i+1 to T5.

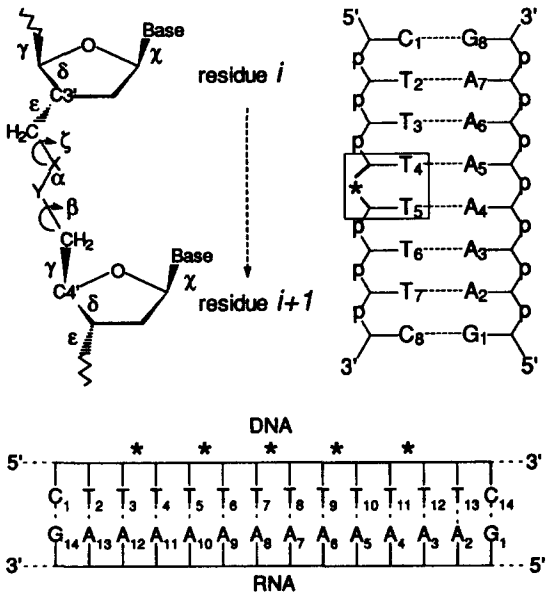

Figure 4. *Top left:* definitions of torsional angles in amide **3** and **4** backbone modified nucleotides. See also legend of Table 1. Residues *i* and *i+1* are residues "above" and "below" an amide-modified backbone portion and are denoted as T_i and T_{i+1}, respectively, throughout the text. *Top right:* octamer RNA·DNA hybrid duplex used for conformational analysis with one amide linkage between residues T4 and T5 (marked by *) in the DNA strand. The conformational analysis is performed on the framed T4*T5 portion. *Bottom:* alternatingly modified 14*mer* RNA·DNA hybrid duplex with five amide linkages (marked by *) in the DNA strand used for molecular dynamics simulations.

For the amide **3** and amide **4** modifications, the enforced torsional angles were ζ(T4) and β(T5), i.e. the dihedrals which do not correspond to the amide bond (i.e. α of T5) or to a bond joined directly to the sugars (see Figure 4). After each torsional enforcement step, the octamer duplex was first minimized with the penalty function of equation 2 included until the maximum derivative was smaller than 0.5 kcal mol^{-1} $Å^{-1}$. All constraints were then removed and the structure was freely relaxed (convergence criteria of 0.1 kcal mol^{-1} $Å^{-1}$). Minimizations were carried out with the conjugate gradient algorithm. This procedure was repeated in steps of 30 degrees until a complete turn was achieved. The same protocol was applied to both amide-modified structures with the amide group in a *trans* and in a *cis* starting conformation.

The conformational analysis protocol above involves the stepwise change of only one torsional angle at a time, with the final minimization step leading to the closest local minimum on the potential energy surface. In order to verify that the protocol scans the entire conformational space efficiently, another procedure was also applied. For each amide modification, the hybrid octamer was submitted to high-temperature MD (1000 K) during 200 picoseconds (ps). Only the two central modified residues T4 and T5 were allowed to move, the other DNA residues and the entire RNA strand being kept fixed to their initial coordinates in order to preserve the overall double-helix structure. Every picosecond, a (highly perturbed) conformation was extracted and the total duplex was relaxed by minimization (with all constraints removed) until the maximum derivative was smaller than 0.1 kcal mol^{-1} $Å^{-1}$. No additional clearly distinct local energy minima were found by this technique, suggesting that the systematic scanning of conformational space by torsional angle enforcement is efficient for this type of structure.

Note that the sugar puckering was rarely affected by the conformational analysis performed by the torsional enforcement procedure. Furanoses usually remained in their initial C3'-*endo* puckering state. Various puckering states were captured during the MD simulations at high temperature. However the rest of the backbone geometry was not dramatically affected by such changes.

Molecular dynamics (MD)

MD Studies were carried out on 14*mer* hybrid duplex structures r[$GA_{12}G$]·d[$CT_{12}C$], the DNA strand of which was modified alternatingly by either the amide **3** or amide **4** linkage, as indicated by * in Figure 4. The alternatingly modified structures were studied because the synthesis of amide-modified DNA sequences involves the incorporation of amide-linked dimers in DNA sequences by standard oligomerization procedures,[22] yielding amide linkages automatically which alternate with wild-type phosphodiesters.

Obviously, relatively short MD trajectories like the 100 ps simulations reported in this paper are highly dependent on the starting situation. Therefore, repeating the simulations with various initial configurations is a prerequisite to understand, at least partially, the dynamic behavior.

Starting geometries for the modified portions were based on the results of the conformational analysis. All low-energy conformers found for the amide-modified portions were used as MD starting structures. The five amide linkages in alternating modified strands were always preset to the same starting conformation. Starting with mixed conformers would lead to an overwhelming number of possibilities. Furthermore, even on a short time scale, low-energy barriers should in principle be overcome, thus yielding "mixed-conformer" sequences automatically.

The structures were first minimized with torsional angle constraints in the modified backbone portions in order to enforce a defined conformation until the maximum derivative was smaller than 0.5 kcal mol^{-1} $Å^{-1}$. Constraints were then removed and the 14*mers* were fully relaxed by minimization down to a derivative of 0.1 kcal mol^{-1} $Å^{-1}$. With this procedure, all the modified residues within the same molecule adopt similar conformations while the unmodified portions remain in the standard DNA conformation. No conformational changes are induced in the RNA strand. It was verified that the minimized conformations of the modified

residues in the alternatingly modified 14*mers* were close to those obtained with the conformational analysis. The minimized duplex structures were then used as MD starting geometries.

MD Simulations were performed in the NVT ensemble keeping the temperature constant at 300 K by coupling to an external heat bath.[23] A time step of one femtosecond was used for the numerical integration. The system was heated progressively from 0 to 300 K over a total period of 24 ps in the following way: 2 ps at 50 K and 100 K, 4 ps at 150 K and 200 K, 5 ps at 250 K, and 7 ps at 300 K. Trajectories for later analysis were then recorded for 100 ps, saving instantaneous frames every 0.5 ps.

Results and Discussion

Conformational analysis

Various conformers were obtained for each amide modification. Tables 1 and 2 summarize the geometries adopted by the modified residues. None of the unmodified residues were affected by the conformational analysis performed on the modified portions. All natural residues kept a conformation close to the initial DNA- or RNA-standard backbone geometry.

For the amide **3** modification, three clearly distinct conformers with the amide group in a *trans* conformation were obtained. One energetically reasonable local minimum was found for the *cis* amide **3** group. The geometrical features of the four lowest-energy minima found for the amide **4** modification (three in *trans* and one in *cis*) are close to those obtained for the amide **3** modification. Three additional local minima were detected with the amide **4** group in a *cis* conformation, two of which are very high in energy (>10 kcal mol^{-1} above the lowest-energy conformation). Figure 5[24] illustrates the conformations adopted by the amide-modified backbone for the four lowest-energy minima found for each modification, called respectively **3a**, **3b**, **3c** and **3d** for the amide **3** linkage, and **4a**, **4b**, **4c** and **4d** for the amide **4** modification.

In Tables 1 and 2 are listed the total AMBER potential energies of the modified octamers and the relative energies as compared to the lowest-energy minimum. Note that these relative energies represent the energy difference between two entire octamer duplexes and not only the difference between two conformations of the amide-modified T4*T5 sequence. Therefore, the relative energy values take into account both the modified backbone conformation and any rearrangement of the entire double-helix structure which may follow from it. However, since neither adjacent residues in the same strand nor in the complementary RNA strand were strongly perturbed during the conformational analysis, the relative energies can be regarded as a good estimate for the conformational energy differences between the various amide backbone conformers. Also, the sugar puckering states were rarely affected during the conformational analysis by torsional angle enforcement, i.e. the potential energies given in Tables 1 and 2 correspond to double helices with sugars of both strands close to their initial C3'-*endo* puckering mode (with $\delta \approx 80°$). Obviously, the potential energy changes to some extent with the puckering mode of the sugars. In fact, the high-temperature dynamics protocol to assess different backbone conformations yielded backbone conformers identical to those listed in Tables 1 and 2, but with sugars adopting differing puckering states. Since the puckering of the furanose rings in nucleic acids is a dynamic process, it is discussed in detail in the subsequent sections dealing with molecular dynamics simulations.

Table 2. Backbone conformations of local minima found for the amide **4** modified octamer r(GA_6G)·d(CTTT*TTTC)

Domain	Energy	Residue	α	β	γ	δ	ε	ζ	χ	amide
4a	–139.0	i	–74	176	61	77	**169**	**–101**	–159	*trans*
	(0.0)	i+1	**171**	**–123**	**169**	79	–160	–64	–170	
4b	–137.4	i	–74	176	60	75	**171**	**72**	–159	*trans*
	(+1.6)	i+1	**–169**	**60**	**168**	78	–155	–63	–175	
4c	–135.2	i	–74	175	63	73	**125**	**80**	–161	*trans*
	(+3.8)	i+1	**–175**	**130**	**80**	72	–171	–67	–159	
4d	–133.6	i	–76	178	56	76	**–172**	**–103**	–157	*cis*
	(+5.4)	i+1	**1**	**124**	**57**	73	–163	–63	–162	
4e	–133.4	i	–76	177	59	74	**82**	**93**	–158	*cis*
	(+5.6)	i+1	**3**	**–139**	**–165**	82	–165	–63	–159	
4f	–128.5	i	–72	178	55	67	**–97**	**–93**	–158	*cis*
	(+10.5)	i+1	**–16**	**68**	**163**	75	–144	–63	180	
4g	–126.6	i	–74	173	63	79	**–84**	**–74**	–166	*cis*
	(+12.4)	i+1	**12**	**–55**	**–133**	85	–168	–63	–155	

See also legend and footnotes to Table 1.

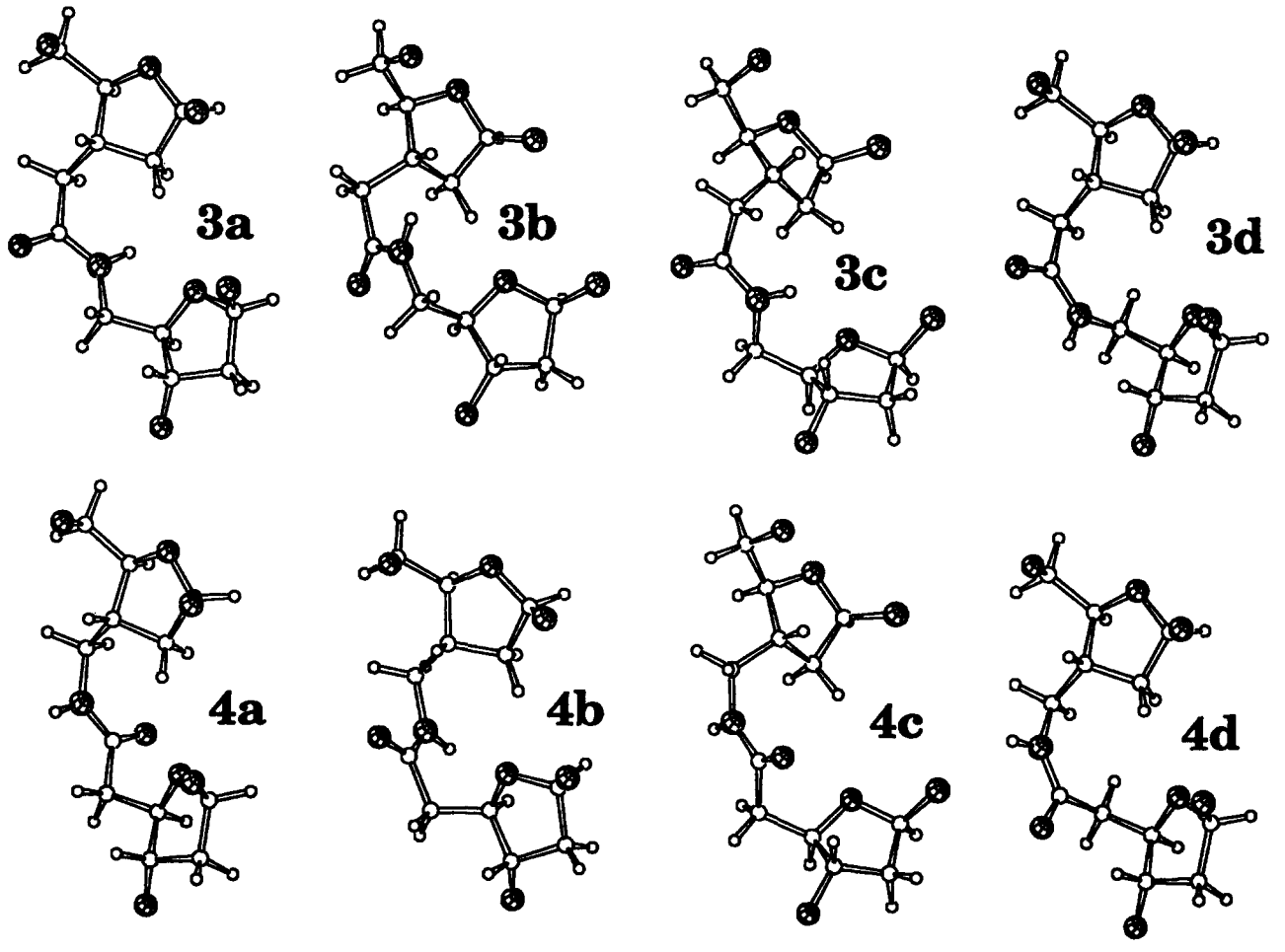

Figure 5. Four lowest-energy conformers found for the amide **3** and amide **4** T4*T5 modified dimers. The represented structures are cut out of the octamer duplex shown framed in Figure 4. For clarity, only atoms N1 of the thymine bases are displayed.

Wild-type oligonucleotides adopt well defined and well characterized duplex structures, especially in the crystalline state. Still, even for natural nucleic acids divergences from the "standard" A- or B-form double helices are observed.[25-30] We have also applied conformational analysis to a wild-type octamer duplex r(GA$_6$G)·d(CT$_6$C). As for the amide-modified octamers, only the central residues T4 and T5 were considered but, in this case, all the backbone torsional angles (α, β, γ, δ, ε, ζ) were successively enforced. Geometries of the four lowest-energy conformers are given in Table 3. As mentioned for the amide-modified octamers, relative energies correspond to energy differences between entire octamer duplex geometries and may be affected by different sugar puckering modes.

It turns out that the three lowest-energy conformers found for the amide **3** and amide **4** modifications are very close to the three "non-standard" lowest-energy conformers found for the unmodified octamer. Thus,

Table 3. Backbone conformations of the four lowest-energy conformers found for the unmodified hybrid octamer r(GA$_6$G)·d(CT$_6$C)

Domain	Energy	Residue	α	β	γ	δ	ε	ζ	χ
1	–136.6	i	–76	175	63	79	–169	–64	–158
	(0.0)	i+1	–75	175	63	79	–169	–64	–157
2	–134.7	i	–76	176	64	82	–176	–66	–155
	(+1.9)	i+1	143	–174	–179	82	–159	–63	–167
3	–132.1	i	–74	176	63	76	171	45	–160
	(+4.5)	i+1	-163	77	170	77	–160	–65	–170
4	–132.1	i	–76	175	60	69	83	70	–158
	(+4.5)	i+1	–155	172	64	79	–177	–69	–143

See also legend and footnotes to **Table 1.**

Table 4. MD behavior of amide-alternating modified 14*mers*: global observations

Modification	Starting Conformation	MD behavior over 100 ps
amide-3	**3a**	all residues kept a **3a** conformation
	3b	4 residues adopted a **3a** conformation
	3c	all residues kept a **3c** conformation
	3d	all residues kept a **3d** conformation
amide-4	**4a**	2 residues adopted a **4b** conformation
	4b	5 residues adopted a **4a** conformation
	4c	3 residues adopted a **4a** conformation, 2 residues adopted a **4b** conformation
	4d	all residues kept a **4d** conformation

amide **3** and amide **4** backbone-modified oligonucleotides are able to adopt duplex geometries which are also conceivable for the unmodified DNA backbone. Furthermore, the major conformational difference between the standard DNA geometry and the geometry of the lowest-energy conformers **3a** and **4a** stems from the torsional angles α(T5) and γ(T5). Both torsional angles adopt a *trans* conformation in the amide-backbone conformation whereas the standard DNA conformation has α in *gauche*$^-$ and γ in *gauche*$^+$. The conformer with α and γ in *trans* corresponds to the second lowest-energy minimum obtained for the unmodified octamer. This variant of the DNA backbone conformation is clearly a low-energy state. It has also been observed in the X-ray structures of A-form DNA·DNA duplexes[25-27] and is commonly noticed as backbone conformational transition in molecular modeling studies on DNA and RNA duplexes.[19,30,31]

Molecular dynamics

Global observations. For both amide modifications **3** and **4**, the four lowest-energy conformers were used as MD starting geometries (three with the amide group in *trans*, namely **a**, **b** and **c**, and one with the amide group in *cis*, i.e. **d** in Tables 1 and 2). As mentioned before, only conformationally homogeneous sequences were used as starting geometries. However, even on the short time scale of 100 ps, low-energy barriers should in principle be surmounted at least in some residues, thus yielding "mixed-conformer" sequences at various instants. This has indeed been observed in several cases, as summarized in Table 4. The transitions from one conformational state to the other on the 100 ps time scale demonstrate that the energy barriers to be overcome on the potential energy surface are in the order of a few *kT* units only. On the other hand, some conformations are clearly trapped in a local minimum situation from which they cannot easily escape. It is important to note that the stochastic nature of a molecular dynamics trajectory may render an evaluation of the frequency of transitions precarious, especially when the actual simulation time is rather short. Thus for example, the finding that the conformer **3a** is conservative on a 100 ps time scale does not imply that the transition from **3a** to any other conformation is in principle excluded. It merely suggests that it is less probable than the transition from **3b** to **3a** or transitions between the various conformers of amide **4**.

In Figure 6 are shown the starting geometries (fully minimized 14*mer* duplexes, top row) and the MD averaged structures (bottom row) for the unmodified RNA·DNA duplex and the amide-modified analogues with amide **3** (in conformations **3a** and **3c**) and amide **4** (in conformation **4a**). The MD averaged structures have the standard Watson–Crick base pair scheme conserved, indicating that the amide modifications lead indeed to geometries comparable to the corresponding wild-type duplex. The same observation was also made for all those duplex structures in which the amide-modified backbones underwent conformational transitions. Thus, the conclusion from the conformational analysis can be extended to the results of the MD simulations: the replacement of the phosphodiester linkage by amide **3** or amide **4** does not appreciably disturb the backbone geometry and standard Watson–Crick base pairing with a complementary RNA strand is feasible without severe distortions.

In Table 5 are listed values for time-averaged torsional angles and sugar puckering parameters together with their standard deviations (in parentheses) for selected residues of the three conformers **3a**, **3b**, and **3c** of amide **3** and of the lowest-energy conformer **4a** of amide **4**. Because of the transitions between the different conformers of amide **4** (see Table 4), selected residues of **4b** and **4c** are not represented in Table 5. Results concerning conformers with the amide group in *cis* have also been excluded from a more detailed analysis. These conformations are conserved during the dynamics despite their relative high energy because the barriers of conversion are too high to allow conformational changes to be observed during a 100 ps trajectory. Similarly, details for the respective complementary RNA strands are not shown. In all amide-modified duplexes, the RNA strands behaved as in the wild-type RNA·DNA duplex.[19] However, data for a selected dimer from the corresponding unmodified ("wild-type") DNA strand are included for comparison.

Table 5. Backbone torsion angles and sugar puckering parameters averaged over 100 ps for selected residues (with standard deviation in parentheses). All values are given in degrees

Conformation[a]	Residue	α	β	γ	δ	ε	ζ	χ	*P*	τ_m
3a	T7	–74 (11)	179 (8)	58 (10)	94 (19)	176 (9)	–100 (18)	–156 (13)	86 (35)	42 (6)
	T8	171 (8)	–149 (24)	173 (9)	107 (25)	–166 (9)	–79 (13)	–154 (17)	103 (43)	42 (6)
3b[b]	T3	–73 (11)	174 (9)	58 (11)	76 (10)	163 (10)	46 (17)	–157 (11)	48 (22)	44 (5)
	T4	–173 (7)	76 (15)	175 (10)	101 (23)	–168 (10)	–75 (12)	–158 (16)	94 (39)	43 (6)
3b[c]	T7	–77 (12)	174 (9)	58 (9)	81 (15)	169 (10)	–8 (93)	–152 (11)	52 (36)	43 (6)
	T8	–178 (11)	132 (68)	174 (8)	103 (25)	–170 (9)	–78 (13)	–154 (18)	96 (44)	42 (6)
3c	T7	–73 (11)	175 (9)	60 (10)	99 (13)	60 (9)	89 (14)	–135 (12)	105 (16)	42 (6)
	T8	180 (9)	164 (20)	69 (10)	100 (15)	–177 (8)	–87 (12)	–134 (17)	103 (23)	44 (5)
4a[d]	T5	–77 (11)	176 (9)	59 (10)	83 (18)	168 (9)	–21 (112)	–155 (12)	58 (36)	43 (5)
	T6	179 (12)	–26 (82)	175 (10)	98 (23)	–165 (9)	–73 (12)	–159 (16)	89 (39)	42 (6)
4a[e]	T7	–78 (11)	174 (9)	59 (10)	84 (16)	169 (9)	–137 (24)	–154 (11)	61 (33)	42 (6)
	T8	171 (9)	–94 (21)	178 (9)	100 (23)	–166 (10)	–76 (13)	–156 (15)	90 (40)	42 (6)
unmodified	T7	–70 (11)	175 (10)	63 (9)	108 (18)	–176 (8)	–89 (12)	–139 (16)	110 (27)	42 (5)
	T8	–70 (12)	176 (10)	62 (11)	108 (17)	–176 (9)	–88 (11)	–140 (15)	112 (26)	42 (6)

[a]All the five amide-linkages are initially in the same conformation. [b]Modified dimer which kept a **3b** conformation over the 100 ps MD trajectory.
[c]Modified dimer which converted from **3b** to **3a** conformation after 61 ps. [d] Modified dimer which converted from **4a** to **4b** after 52 ps. [e]Modified dimer which kept a **4a** conformation over the 100 ps MD trajectory.

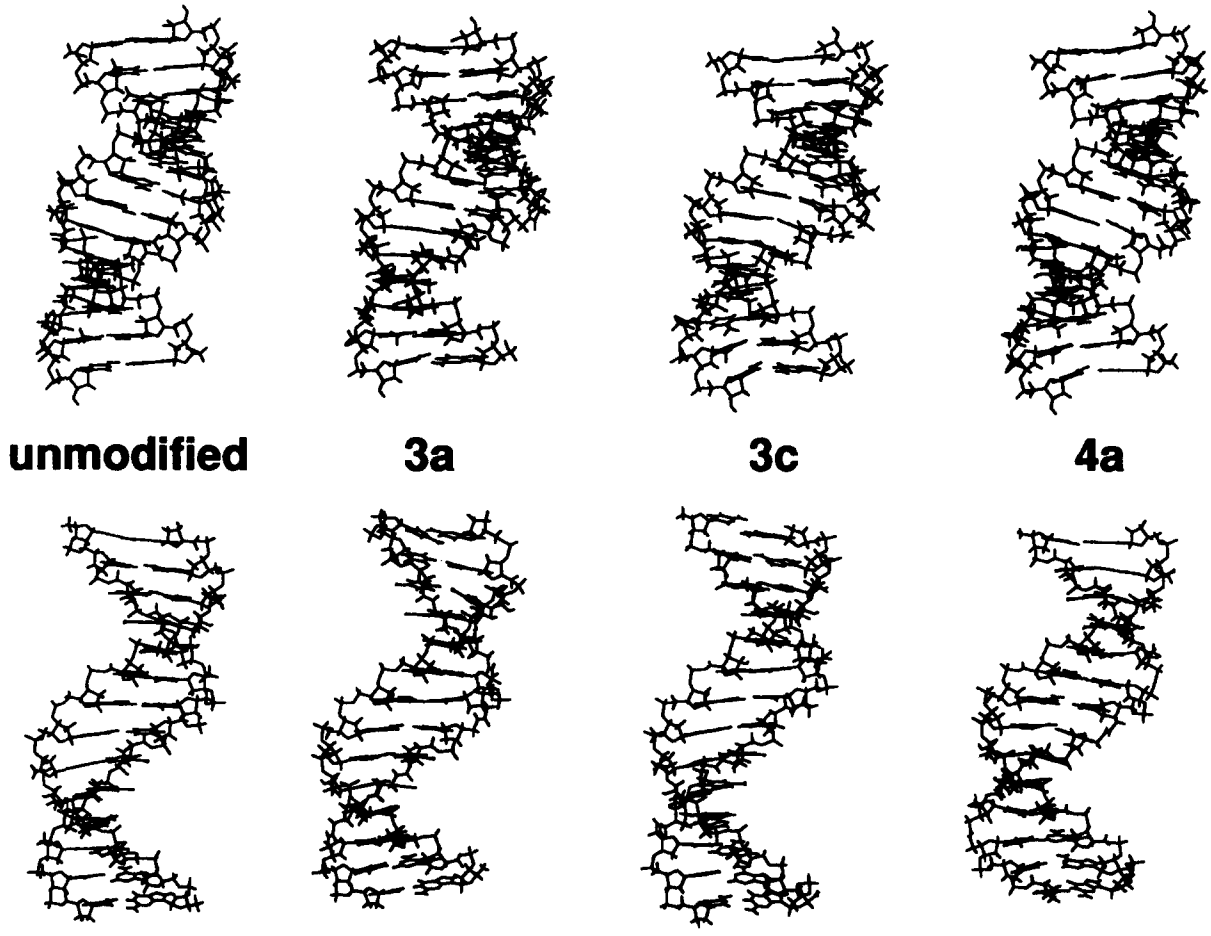

Figure 6. Fully minimized MD starting structures (top row) and MD average structures (bottom row) of the wild-type RNA·DNA hybrid duplex and alternatingly modified 14*mers* with amide linkages **3** (in starting conformations **3a** and **3c**) and **4** (in starting conformation **4a**).

Backbone transitions. As indicated in Table 4, all modified residues with the starting conformation **3a** were found to oscillate around the starting structure. No conformational transitions were observed in the backbone during the 100 ps simulation. The conservative behavior is evidenced by the small standard deviations of the backbone torsional angles in Table 5. With the conformation **3b** as starting geometry, four out of five amide residues converted back to the **3a** conformation during the same simulation period (T5*T6 after 7 ps, T7*T8 after 61 ps, T9*T10 after 88 ps, and T11*T12 after 40 ps). Because of the rigidity of the amide group, the **3b** → **3a** transition requires the simultaneous change of the torsional angle pair [$\xi(T_i)$, $\beta(T_{i+1})$] from a [g^+, g^+] conformation to a [g^-, ~t] conformation. Such a transition is illustrated for the amide linkage T7*T8 at the top of Figure 9 (see later for a more detailed discussion). The only modified dimer keeping a **3b** conformation over the whole MD simulation, i.e. T3*T4, is also entered in Table 5. It differs from the T7*T8 dimer by the average values and the smaller standard deviations for the two angles ζ and β. For conformer **3c** all torsional angles remained trapped in the conformational domains of the starting geometry.

The amide-linked dimer T7*T8 of amide **4** in starting conformation **4a** remained in its initial conformation. The dimer T5*T6 is included in Table 5 as an example of a **4a** → **4b** transition which is indicated by the large standard deviations of torsional angles ζ and β.

Complementary RNA strands behaved similar in all cases, the only momentary backbone transition in the RNA strand being the sometimes observed [g^-, g^+] → [t, t] for the angle pair [α, γ].[19]

Sugar puckering. The last two columns in Table 5 list the average puckering parameters P and τ_m and their corresponding standard deviations. The alternating character of the modified strands has an interesting side-effect on the sugar puckering behavior. There are two types of furanoses, one with the amide linkage attached at the C3', i.e. "above" the amide and denoted T_i hereafter (residue i in Figure 4) and one attached to the amide via C5', i.e. "below" the amide and called T_{i+1} from now on (residue $i+1$ in Figure 4). These distinct sugars can have clearly different puckering schemes.

In Figure 7 distributions of puckering modes are shown, recorded over 100 ps every 0.5 ps. The values are

averaged over the ten "inner" residues of the duplexes, i.e. thymine residues T3 to T12 in the DNA strands and the complementary adenine residues in the RNA strands (see Figure 4). Thus, 2000 data points were used in each histogram. In order to illustrate the relative contributions of the T_i and the T_{i+1} sugars to the overall distribution, the respective separate histograms (including 1000 data points each) are also shown (diagrams on the right in Figure 7). In Table 6 are listed the corresponding statistics in numbers (averages, standard deviations, and extremes).

The histograms for the unmodified RNA·DNA hybrid duplex are in perfect agreement with earlier published data, obtained with the original AMBER partial charges.[19] Also, these data on the puckering behavior reproduce accurately recent NMR studies of RNA·DNA hybrid duplexes.[32–35] The riboses of the RNA strand adopt an average C3'-*endo* puckering mode with moderate oscillations while the deoxyriboses of the DNA strand pucker continuously between the classical C3'-*endo* and C2'-*endo* states, resulting in an average puckering domain of O4'-*endo* to C1'-*exo*. Obviously, all

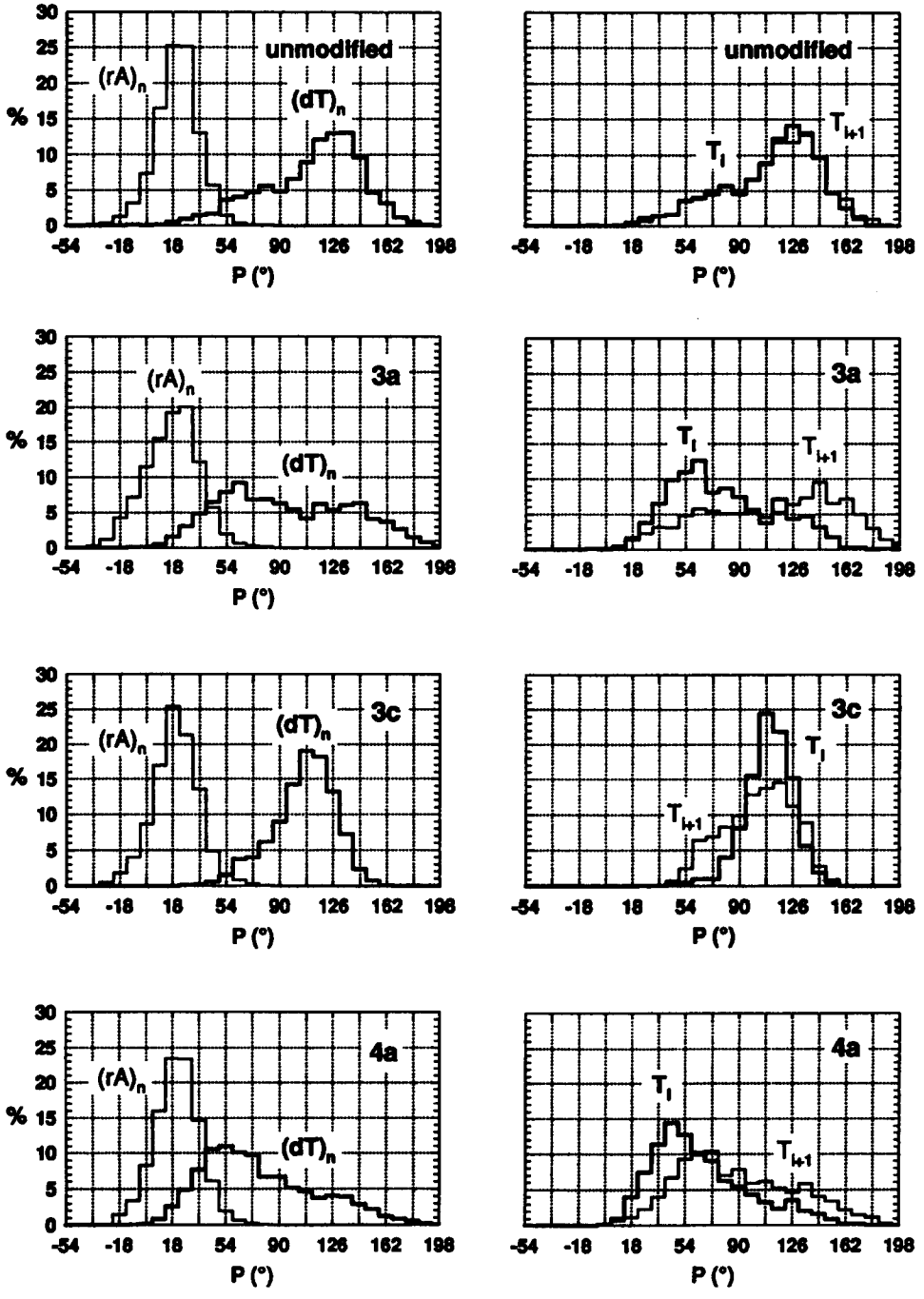

Figure 7. *Left*: histograms of puckering states of adenine residues A3–A12, respectively thymine residues T3–T12 in the unmodified and amide-modified 14*mers* recorded over 100 ps in steps of 0.5 ps (i.e. 2000 data points for each strand). *Right:* separate histograms for the residues T_i and T_{i+1} (see text for details).

Table 6. Analysis of sugar puckering statistics for the ten inner residues over 100 ps, data collected every 0.5 ps. All values are given in degrees

Duplex structure	Mean values of phase angle of pseudorotation P over ten inner residues		Mean values of phase angle of pseudorotation P and extreme values P_{min}, P_{max} in DNA strands subdivided according to T_i sugars and T_{i+1} sugars					
	A_9–A_{12} residues in RNA strand	T_3–T_{12} residues in DNA strand	Puckering of T_i sugars (T_3, T_5, T_7, T_9, T_{11})			Puckering of T_{i+1} sugars (T_4, T_6, T_8, T_{10}, T_{12})		
			P	P_{min}	P_{max}	P	P_{min}	P_{max}
unmodified[a]	16 (15)	107 (33)	107 (33)	–14	234	107 (33)	–14	234
3a-modified DNA strand	13 (18)	90 (43)	74 (34)	–12	189	106 (46)	–9	194
3c-modified DNA strand	15 (16)	102 (21)	105 (17)	26	153	98 (24)	25	160

[a]In unmodified strands, all thymine residues are equivalent. Values for T_i and T_{i+1} residues are identical and were taken considering all ten inner residues of the 14*mer*.

sugars in the unmodified DNA strand are equivalent (as are the histograms for T_i and T_{i+1}) and the artificial splitting into T_i and T_{i+1} is just done for comparison with the modified strands.

The histograms for the amide **3** modified DNA strand with amide linkages in the **3a** conformation are clearly different from the corresponding distribution of the unmodified duplex. There are two distinct peaks in the distribution of puckering states. The two peaks stem from the individual histograms of the T_i and the T_{i+1} sugars, the shapes of the distributions being almost mirror images. The splitting into individual contributions demonstrates that the T_i and the T_{i+1} sugars have a clearly different puckering behavior. The average value of P is 74° for T_i residues and 106° for T_{i+1} residues. (Note that these values refer to all T_i, respectively T_{i+1} residues, in contrast to the values in Table 5, which refer to a defined T_i–T_{i+1} dimer sequence only.)

The effect of the backbone conformation on the sugar puckering is explicitly evidenced by comparing the puckering distribution for the **3c** conformation with that of the **3a** conformation. For **3c** both the T_i and the T_{i+1} sugars pucker similarly. The individual histograms representing the respective distributions have the maxima around the same value of P. The overall histogram for the puckering distribution of the modified DNA strand with the amide linkage in conformation **3c** resembles that of the unmodified hybrid duplex, although the distribution is more symmetric and narrower and although the maximum is slightly shifted to a smaller P value.

Because four out of five residues converted to the **3a** conformation during dynamics, histograms calculated over all residues for modified duplex with **3b** conformations are not shown. For the single dimer T3*T4 which did not convert from **3b** to **3a**, the average puckering states over the 100 ps trajectory stem from two distinct distributions, one broad (T4, a T_{i+1} residue) covering almost the entire puckering spectrum from C3'-*endo* to C2'-*endo*, the other one narrow (T3, a T_i residue) and culminating around P = 45° (see Figure 8).

Similarly, the analysis of the puckering distribution for amide **4** is rendered difficult because of continuous transitions between the various backbone conformations which influence the sugar puckering. In Figure 7 are shown the resulting histograms when starting from the **4a** conformation, neglecting the fact that two residues converted to **4b** during the simulation. The individual histograms for the residues T_i and T_{i+1} visualize the

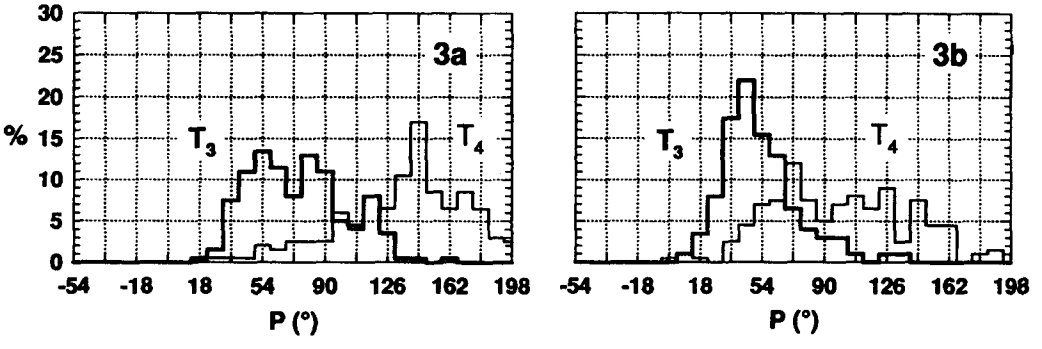

Figure 8. Histograms of puckering states for the dimers T3*T4 in the case of the **3a** and **3b** conformations. T3*T4 is an example amide-linked portion which did not convert from **3b** to **3a** in 100 ps of dynamics trajectory (see also text and legend of Figure 7).

distinct behavior of the respective sugars. Differences with respect to the amide **3** modified duplexes (in any starting conformation) are obvious.

Puckering histograms for the RNA strands are very similar in all cases. As for the backbone, the puckering states in the RNA strands are not strongly affected by the nature of the complementary strands.

Overall, the average values of *P* in the amide modified strands are lower (i.e. closer to northern (N) puckering) than in the corresponding wild-type RNA·DNA duplex. Furthermore, *P* values for the T_i sugars are smaller than for the T_{i+1} sugars, at least in the lowest-energy conformations. The finding that the T_i sugars tend more to northern (N) puckering might be explained, at least partially, by the length and especially the rigidity of the amide linkage. The amide linkage seems to push the C3' atom of residue T_i "upward", inducing a trend towards N puckering. The torsional angle towards the base χ is correlated with *P*. Whereas χ assumes a value around −140° in the unmodified duplex, χ becomes ≈ −155° in the amide-modified strands. An exception is observed for the **3c** conformer. In this case, *P* values are close to those of the unmodified duplex, there is no sizable difference for the T_i and T_{i+1} residues, and also the torsional angle χ assumes the same value as in the wild-type structure.

Correlation of sugar puckering and backbone conformation. As seen above, the puckering of the sugars depends not only on the structural isomers, but also on the conformation of the amide-modified backbone portions. For both the **3a** and the **3b** conformer, the T_i sugars are found to adopt a definitely lower average value for *P* than the T_{i+1} sugars. However, the difference is far more pronounced in the case of the **3b** conformer. For the dimer T3*T4, i.e. the only one that stayed **3b** over the entire MD trajectory, the T3 (T_i) sugar oscillates around $P = 45°$ which corresponds to a puckering mode between C3'-*endo* and C4'-*exo*. The T4 (T_{i+1}) sugar assumes O4'-*endo* on average stemming from a continuous oscillation between C3'-*endo* and C2'-*endo*. Upon transition from backbone conformation **3b** to **3a**, the puckering behavior changes. This is shown graphically in Figure 9 (bottom) for the amide-linked dimer T7*T8. It can be seen that the T8 (T_{i+1}) sugar (dotted curve) puckers more or less freely between the C3'-*endo* and C2'-*endo* domains (indicated by the dashed horizontal lines at $P = 18°$ and at $P = 162°$) over the entire 100 ps trajectory. On the other hand,the T7 (T_i) sugar (solid curve) is quite constrained to the puckering range of $P = 0$–$90°$ as long as the amide linkage is in the **3b** conformation. At 61 ps (indicated by the vertical line), the transition to the **3a** conformer frees the T_i sugar from its constraint and it now oscillates over a larger puckering range.

Although the **3a** conformation was found to be slightly favored energetically over the **3b** conformation (see Table 1), the small potential energy difference alone cannot be made responsible for the absence of **3a** → **3b** transitions on the 100 ps time scale, noting that the barrier of conversion can be readily overcome (as evidenced by the **3b** → **3a** under identical conditions). The broader range of allowed puckering induced by the

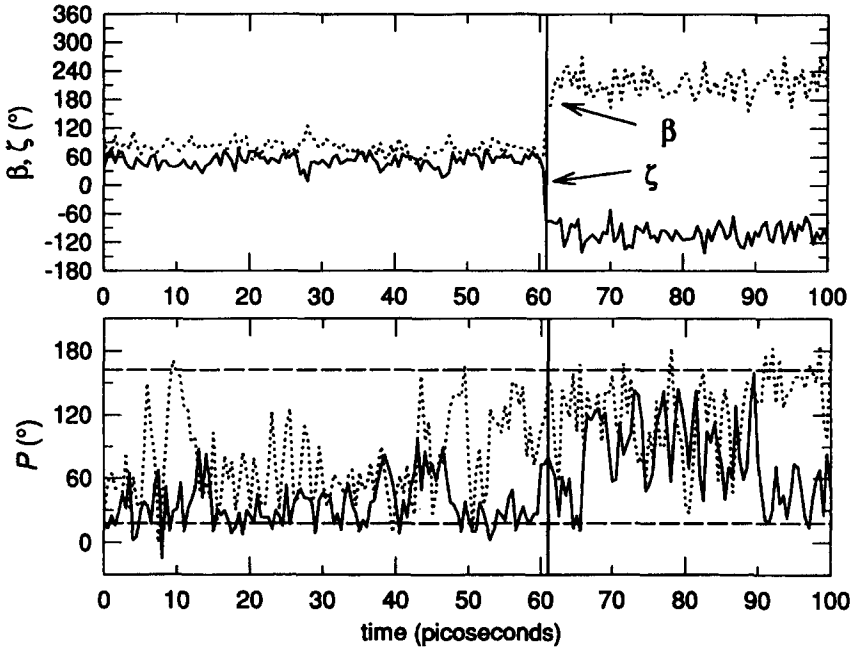

Figure 9. *Top:* Conformational transition **3b** → **3a** observed in a 14*mer* duplex alternatingly modified by amide **3** linkages. All amide linkages were initially in **3b**. The transition (occurring after 61 ps in this case, see vertical line) requires the simultaneous change of the torsional angles $\xi(T_i)$ and $\beta(T_{i+1})$ from a $[g^+, g^+]$ to a $[g^-, \sim t]$ conformation. *Bottom:* phase angle of pseudorotation *P* of the T_i sugar (solid line) and of the T_{i+1} sugar (dotted line).

transition from **3b** to **3a** increases the number of states that the system can assume, i.e. the entropy. Therefore, the **3a** conformation seems to be favored for free energy reasons.

If these considerations are correct, the **3a** → **3b** transition should be observed when the T_i sugar is artificially restricted in its puckering freedom because this would remove the "excess entropy" in the **3a** conformation. In order to test this hypothesis, an additional MD simulation was run with an amide **3** modified 14*mer* duplex, starting with the five amide linkages in the **3a** conformation. However, all T_i sugars were constrained to the C3'-*endo* puckering range. This was achieved by enforcing the torsional angle δ in the T_i furanoses to 80° by using an additional harmonic force field term as in equation 2, with a force constant k_{enf} = 1000 kcal mol^{-1} rad^{-2}. In this constrained simulation, two out of five **3a** conformers switched to **3b** and back to **3a** on the 100 ps time scale, indicating that there is no distinct preference for either conformer once the sugar puckering freedom is removed artificially in conformer **3a**. A **3a** → **3b** → **3a** transition is shown in Figure 10. The top plot shows the simultaneous changes of ζ in T_i and β in T_{i+1} as a function of time. The plot below displays the corresponding oscillations of the phase angle of pseudorotation *P*. The T_i sugar (solid curve) is restricted to the 0–90° domain (as a consequence of the artificial constraint on δ) while the T_{i+1} sugar oscillates more freely over the whole C3'-endo to C2'-endo range.

The correlation between sugar puckering and backbone conformation as shown above is an example of the complexity of nucleic acid structures and their analogues. The various parts are not behaving independently but their accessible states are strongly correlated. Transitions in the backbone induce changes in the puckering scheme and vice versa.

Conclusions

The replacement of the phosphodiester linkage in oligonucleotides by the amide backbones **3** or **4** (Figure 1) leads to a new type of hybrid RNA·DNA duplex. It has been established experimentally that the amide-modified DNA sequences can form sequence-specific duplexes with a complementary RNA strand. Melting points of the modified duplexes are similar to those of the corresponding wild-type structures. In some instances, even a slight stabilization is noted.[10,11] Furthermore, the amide-modified DNA sequences are found to be considerably more resistant towards nucleases, making them suitable candidates for antisense technology.

The computer simulations in this study corroborate the concept that the amide-modified backbones with modifications **3** and **4** shown in Figure 1 can assume conformations which still allow Watson–Crick base pairing without severe geometrical distortions.

Conformational analysis has shown that several conformations are accessible to both amide linkages without disruption of the double helix structure. The backbone geometry of the four lowest-energy conformers are similar for both amide modifications. The lowest-energy conformers found in each case only differ from the standard DNA-backbone geometry by a

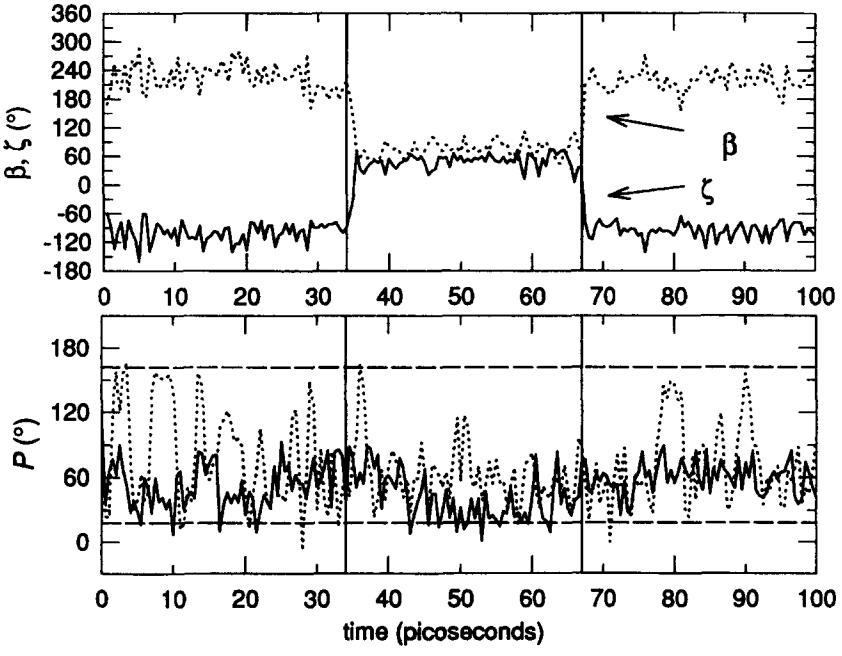

Figure 10. *Top:* Conformational transition **3a** → **3b** → **3a** observed in a 14*mer* duplex alternatingly modified by amide **3** linkages. The transition from **3a** to **3b** was obtained after constraining the puckering amplitude of the T_i sugar. Transitions are marked by the vertical lines. *Bottom:* phase angle of pseudorotation *P* of the T_i sugar (solid line) and of the T_{i+1} sugar (dotted line). See also legend of Figure 9 and text.

[*t*, *t*] conformation of the torsional angle pair [α, γ] which appears to be a low-energy variation of the standard DNA [*g*-,*g*+] arrangement even found in X-ray structures of wild-type DNA.[25-27]

Molecular dynamics studies have revealed that various conformers can interconvert on a 100 ps time scale, indicating that the barriers of transition are rather low. In general, the puckering of the deoxyriboses attached directly to an amide linkage is more shifted to N puckering, i.e. closer to the puckering mode of A-type DNA. This is in contrast to wild-type RNA·DNA duplexes in which the DNA strand oscillates between the A-type C3'-*endo* and the B-type C2'-*endo* puckering domains. Furthermore, the MD investigations have shown that in alternatingly modified sequences (as resulting from the chemistry involved in the synthesis of the amide-modified backbones), two distinct types of furanoses appear: a T_i sugar (see Figure 4) with the amide-modified portion attached at C3', and a T_{i+1} sugar, having the amide linkage connected to C4'. The two types of furanoses assume different puckering schemes. The T_i sugars tend more to northern (N) puckering than the T_{i+1} sugars.

The influence of the backbone conformation on the sugar puckering observed in these studies underlines the strong correlation between all different structural entities in nucleic acids and analogues. This fact has to be considered especially in the conception of new antisense oligonucleotides where chemical modifications to various parts of the molecules (backbone, sugar and base) may induce unpredictable effects on other portions of the structures.

Acknowledgments

The authors thank Professor A. Eschenmoser (Laboratorium für Organische Chemie, ETH Zürich, Switzerland) and Professor U. W. Suter (Institut für Polymere, ETH Zürich, Switzerland) for helpful discussions and comments.

References

1. Uhlmann, E.; Peyman, A. *Chem. Rev.* **1990**, *90*, 543.

2. Crooke, S. T. *Ann. Rev. Pharmacol. Toxicol.* **1992**, *32*, 329.

3. Cook, P. D. *Anti-Cancer Drug Design* **1991**, *6*, 585.

4. Milligan, J. F.; Matteucci, M. D.; Martin, J. C. *J. Med. Chem.* **1993**, *36*, 1923.

5. Varma, R. S. *Synlett* **1993**, 621.

6. Vasseur, J.-J.; Debart, F.; Sanghvi, Y. S.; Cook, P. D. *J. Am. Chem. Soc.* **1992**, *114*, 4006.

7. Jones, R. J.; Lin, K. Y.; Milligan, J. F.; Wadwani, S.; Matteucci, M. D. *J. Org. Chem.* **1993**, *58*, 2983.

8. Lebreton, J.; De Mesmaeker, A.; Waldner, A.; Fritsch, V.; Wolf, R. M.; Freier, S. M. *Tetrahedron Lett.* **1993**, *34*, 6383.

9. De Mesmaeker, A.; Lebreton, J.; Waldner, A.; Fritsch, V.; Wolf, R. M.; Freier, S. *Synlett* **1993**, 733.

10. De Mesmaeker, A.; Waldner, A.; Lebreton, J.; Hoffmann, P.; Wolf, R. M.; Freier, S. M. *Angew. Chem. Int. Ed. Engl.* **1994**, *33*, 226. For experimental details on an alternatingly amide **3** modified duplex, see also: Lebreton, J.; Waldner, A.; Lesueur, C.; De Mesmaeker, A. *Synlett* **1994**, 137.

11. Lebreton, J., Waldner, A.; Fritsch, V.; Wolf, R. M.; De Mesmaeker, A. *Tetrahedron Lett.* **1994**, *35*, 5225.

12. De Mesmaeker, A.; Lebreton, J.; Waldner, A.; Fritsch, V.; Wolf, R. M. *Bioorg. Med. Chem. Lett.* **1994**, *4*, 873.

13. De Mesmaeker, A.; Waldner, A.; Lebreton, J.; Fritsch, V.; Wolf, R. M. In: *Carbohydrate Modifications in Antisense Research*, pp. 24–39, Cook, P.D.; Sanghvi, Y.S., Eds; ACS Symposium Series 580; American Chemical Society; Washington, DC, 1994.

14. Weiner, S. J.; Kollman, P. A.; Nguyen, D. T.; Case, D. A. *J. Comp. Chem.* **1986**, *7*, 230.

15. Weiner, S. J.; Kollman, P. A.; Case, D. A.; Singh, U. C.; Ghio, C.; Alagona, G.; Profeta, S.; Weiner, P. *J. Am. Chem. Soc.* **1984**, *106*, 765.

16. Whitlow, M.; Teeter, M. M. *J. Am. Chem. Soc.* **1986**, *108*, 7163.

17. Orozco, M.; Laughton, C. A.; Herzyk, P.; Neidle, S. *J. Biomol. Struct. Dyn.* **1990**, *8*, 359.

18. Ferentz, A. E.; Wiorkiewicz Kuczera, J.; Karplus, M.; Verdine, G. L. *J. Am. Chem. Soc.* **1993**, *115*, 7569.

19. Fritsch, V.; Wolf, R. M. *J. Biomol. Struct. Dyn.* **1994**, *11*, 1161.

20. Rao, S. T.; Westhof, E.; Sundaralingam, M. *Acta Cryst.* **1981**, *A37*, 421.

21. IUPAC-IUB, J. *Eur. J. Biochem.* **1983**, *131*, 9.

22. Gait, M. J. *Oligonucleotide Synthesis: A Practical Approach*, IRL Press; Oxford, 1984.

23. Berendsen, H. J. C.; Postma, J. P. M.; van Gunsteren, W. F.; DiNola, A.; Haak, J. R. *J. Chem. Phys.* **1984**, *81*, 3684.

24. Drawings with Schakal by Keller, E., Insitute for Crystallography, University of Freiburg i.Br., Germany.

25. Frederick, C. A.; Quigley, G. J.; Teng, M. K.; Coll, M.; van der Marel, G. A.; van Boom, J. H.; Rich, A.; Wang, A. H. J. *Eur. J. Biochem.* **1989**, *181*, 295.

26. Ramakrishnan, B.; Sundaralingam, M. *Biochemistry* **1993**, *32*, 11458.

27. Ramakrishnan, B.; Sundaralingam, M. *J. Mol. Biol.* **1993**, *231*, 431.

28. Shakked, Z.; Rabinovich, D. *Prog. Biophys. Molec. Biol.* **1986**, *47*, 159.

29. Kennard, O.; Hunter, W. N. *Quaterly Rev. Biophys.* **1989**, *22*, 327.

30. Sanghani, S. R.; Lavery, R. *Nucl. Acids Res.* **1994**, *22*, 1444.

31. Fritsch, V.; Ravishanker, G.; Beveridge, D. L.; Westhof, E. *Biopolymers* **1993**, *33*, 1537.

32. Fedoroff, O. Y.; Salazar, M.; Reid, B. R. *J. Mol. Biol.* **1993**, *233*, 509.

33. Salazar, M.; Fedoroff, O. Y.; Miller, J. M.; Ribeiro, N. S.; Reid, B. R. *Biochemistry* **1993**, *32*, 4207.

34. Salazar, M.; Champoux, J. J.; Reid, B. R. *Biochemistry* **1993**, *32*, 739.

35. Lane, A. N.; Ebel, S.; Brown, T. *Eur. J. Biochem.* **1993**, *215*, 297.

(*Received in U.S.A.* 7 *September* 1994; *accepted* 19 *January* 1995)